



Published in final edited form as:

*J Biomed Mater Res B Appl Biomater*. 2006 May ; 77(2): 234–240.

## Interfacial Chemistry of Moisture-Aged Class II Composite Restorations

Paulette Spencer<sup>1,2</sup>, Yong Wang<sup>1</sup>, and Brenda Bohaty<sup>2</sup>

<sup>1</sup> Department of Oral Biology, University of Missouri–Kansas City, School of Dentistry, Kansas City, Missouri

<sup>2</sup> Department of Pediatric Dentistry, University of Missouri–Kansas City, School of Dentistry, Kansas City, Missouri

### Abstract

Under *in vivo* conditions, the adhesive/dentin bond at the gingival margin of class II composite restorations can be the first defense against substances that may penetrate and ultimately undermine the composite restoration. Deterioration of this bond during aqueous aging is an area of intense investigation, but to date, the majority of our techniques have provided only an indirect assessment of the degrading components. The purpose of this study was to analyze the *in situ* molecular structure of adhesive/dentin interfaces in class II composite restorations, following aging in aqueous solutions. Class II preparations were cut from 12 unerupted human third molars, with a water-cooled, high-speed, dental handpiece. The prepared teeth were randomly selected for restoration with single bond (SB) and Z100 (3M). Teeth were restored, as per the manufacturer's directions, under environmental conditions that simulated humidity and temperature characteristics of the oral cavity. Restored teeth were kept in sterile Delbecco's phosphate saline for 48 h or 90 days. The samples were sectioned occlusogingivally and micro-Raman spectra were acquired at ~1.5  $\mu\text{m}$  spatial resolution across the composite/adhesive/dentin interfaces at the gingival margins. Samples were wet throughout spectral acquisition. The relative intensity of bands associated with the adhesive in the interfacial region decreased dramatically after aqueous storage. This decrease in concert with the similar depth of dentin demineralization provides direct spectroscopic evidence of leaching of adhesive monomer from the interface during the 90 days of storage. SB adhesive infiltrated 4–5  $\mu\text{m}$  of 12- $\mu\text{m}$  demineralized dentin at the gingival margin. After 90 days of aqueous storage, SB adhesive infiltration was reduced to ~2  $\mu\text{m}$ , leaving ~10  $\mu\text{m}$  of demineralized dentin collagen exposed at the gingival margin. The unprotected collagen at the gingival margin of the aged class II composite restorations was disorganized, suggesting hydrolysis of the collagen, with 90 days of aqueous storage.

### Keywords

dentin; adhesive; degradation; Raman spectroscopy

### INTRODUCTION

Replacement of failed restorations accounts for nearly 75% of operative dentistry,<sup>1,2</sup> and this emphasis on replacement therapy is expected to grow, as the public's concern about mercury release from dental amalgam forces dentists to select alternative restorative materials, for example, composite resin. The failure rate for large to moderately sized posterior composite

---

Correspondence to: P. Spencer or Y. Wang (e-mail: Spencerp@umkc.edu or Wangyo@umkc.edu).

Contract grant sponsor: USPHS Research Grant, The National Institute of Dental and Craniofacial Research, National Institutes of Health, Bethesda, MD; contract grant numbers: DE14392, DE015281, and 1K23DE/HD00468 © 2005 Wiley Periodicals, Inc.

restorations can be 2–3 times high than that of copper amalgam.<sup>3</sup> The higher failure rate of the composite restoration means increased frequency of replacement, with loss of additional tooth structure, that is, sound tooth structure is inevitably removed with each replacement.<sup>4,5</sup>

The premature failure of moderate to large composite restorations can be traced to a breakdown of the bond at the tooth surface/composite material interface<sup>3,6,7</sup> and increased levels of the cariogenic bacteria, *Streptococcus mutans*, at the perimeter of these materials.<sup>8,9</sup> The breakdown of this bond has been linked to the failure of our current materials to consistently seal and adhere to the dentin.<sup>10</sup> Acid-etching provides effective mechanical bonding between the composite restoration and treated enamel, but breakdown at the dentin surface continues to threaten the long-term viability of large posterior composite restorations.<sup>7,8,11</sup> Failure of the bond formed at the interface between the dentin and adhesive allows bacterial enzymes, oral fluids, and bacteria to infiltrate the spaces between the tooth and composite, undermining the restoration and leading to recurrent caries, hypersensitivity, and pulpal inflammation.<sup>12–14</sup>

Recent studies have identified the hybrid layer as the weakest link in the bond formed between the adhesive and dentin.<sup>15</sup> This characterization is based on the results of several laboratory investigations that suggest that the hybrid layer is unstable in aqueous environments.<sup>15–17</sup> It is quite likely that this degradation is related to several factors, including incomplete adhesive infiltration of the demineralized dentin,<sup>18–22</sup> which leads to zones of exposed collagen fibrils within the hybrid layer. The resultant exposed collagen could breakdown in aqueous environments, undermining the integrity of the hybrid layer, the adhesive/dentin bond, and ultimately, the composite restoration.

The majority of investigators have relied on bond strength studies in combination with morphologic examination, to identify the myriad of factors that affect bonding at the adhesive/dentin interface. These techniques assess adhesive/dentin reactions primarily at the point of fracture. Bond strength measurements and the associated fractographic analyses of specimens stored in aqueous solutions provide evidence of deterioration, but these analyses do not permit direct identification of the degrading components. The loss of bond strength over time could be due to deterioration of the resin or degradation of the collagen that was not fully enveloped by the adhesive resin. Authors of previous publications<sup>23,24</sup> have reported that many esterases can degrade methacrylate polymers over time. To date, there has been no investigation of chemical changes that occur within the hybrid layer during storage. The purpose of this study was to compare the molecular structure at the adhesive/hybrid layer/dentin interface in class II composite restorations over time in aqueous storage.

## MATERIALS AND METHODS

### Class II Restoration Preparation

Extracted unerupted human third molars, stored at 4°C in 0.9% w/v NaCl, containing 0.002% sodium azide, were used in this study. The teeth were collected after the patients' informed consent was obtained under a protocol approved by the UMKC adult health sciences institutional review board. As shown in Figure 1, the specimen preparation proceeded as follows: Class II preparations were cut from 12 unerupted third molars, using a high-speed dental drill, with copious water cooling. The occlusal portion was 1.5–2.0 mm wide and 1.0 mm deep in the dentin, and the cervical margin of the proximal box was situated at the cementum–enamel junction. The box was prepared with a bucco-lingual width of 3.0–3.5 mm at the gingival wall and 2.0–3.0 mm at the occlusal wall. The bonding and restoration of the cavity preparations were completed using single bond (SB) adhesive and Z100 composite (3M ESPE, St. Paul, MN, USA), as per the manufacturer's instructions, under environmental conditions that simulated humidity and temperature characteristic of the oral cavity (at 37°C

and 90% humidity). The prepared specimens were etched with 35% phosphoric acid gel (15 s) and rinsed with water, excess water is removed, but the dentin surface remains visibly moist. The composition of SB adhesive include 2,2-bis[4(2-hydroxy-3-methacryloyloxy-propyloxy)-phenyl] propane (BisGMA), 2-hydroxyethyl methacrylate (HEMA), polyalkenoic acid polymer, and ethanol; camphoroquinone and dihydroxyethyl-*p*-toluidine are included as photoinitiators. The adhesive is applied and polymerized for 30 s by exposure to visible light (Spectrum light, Dentsply, Milford, DE, USA). Composite is adapted to the preparation in 1-mm increments, and each increment is polymerized by exposure to visible light for 60 s.

The restorations were finished using fine diamond burs and sofex discs (3M ESPE). Prepared teeth were randomly divided into two groups, that is, six teeth per group. The restored teeth were stored at 37°C (shaking) in sterile Delbecco's phosphate buffered saline (pH 7.0), with 5 mM sodium azide for either 48 h or 90 days. To reduce the possibility of bacterial growth in the vials, the solution was changed biweekly. Following storage for either 48 h or 90 days, the samples were cleaned with distilled water and sectioned occlusogingivally through the proximal box by means of a water-cooled, low-speed, diamond saw (Buehler, Lake Bluff, IL, USA) [Figure 1(A)]. These sections provided representative interfaces from the gingival seat of the proximal box. Then, ~1-mm thick crosssection specimens of the composite/adhesive/dentin interface were used for micro-Raman spectroscopic analysis.

### Micro-Raman Spectroscopy

The composite/adhesive/dentin interface specimens were mounted and covered with distilled water, in preparation for micro-Raman spectroscopic analysis. Raman spectra were recorded using a Jasco NRS-2000 Raman spectrometer, which consisted of an argon ion laser beam (514.5 nm), and focused through a 60× Olympus Plan Neofluor water-immersion objective (NA, 1.2) to an ~1.5 μm beam diameter. Raman backscattered light was collected through the objective and resolved with a monochromator. The spectra were recorded with a liquid nitrogen-cooled CCD detector. The slit width of the spectrograph was set at 140 μm, providing a spectral resolution of 8 cm<sup>-1</sup>. Spectra were recorded at positions corresponding to 1-μm intervals across composite/adhesive/dentin interface, two consecutive scans of spectra (with 60 s accumulation time each) were obtained from each site. The laser power was ~3 mW, and no thermal damage of the tissue specimens was observed during measurement. Spectra were Raman-shift-frequency-calibrated using known lines of neon and silicon.

Each composite/adhesive/dentin slab was mounted at the focus of the objective and covered with distilled water, in preparation for micro-Raman spectroscopic analysis. Spectra were acquired at positions corresponding to 1-μm intervals, across the adhesive/dentin interface, with the use of the computer-controlled xyz stage, with a minimum step width of 50 nm. Multiple sites across the interface at the gingival margins of each specimen were examined spectroscopically.

## RESULTS

The light microscopic image of the adhesive/dentin interface at the gingival margin of a representative class II composite restoration is shown in Figure 1(B). As noted in this image, the interface is very irregular and gaps are readily identified at the gingival margin. In the photomicrographs of a 5-μm thick Goldner's trichrome-stained section of the adhesive/dentin interface [Figures 1(C,D)], the mineralized dentin is green, while the adhesive appears as a very pale color [Figure 1(D)]. An irregular, distinct red region at the gingival margin is visible in Figure 1(D). The red color represents unprotected collagen at the adhesive/dentin interface that was available for reaction with the trichrome stains. Using a 60× water immersion lens, the sample was imaged and Raman spectra were acquired at 1-μm intervals across the composite/adhesive/dentin interface. Representative spectral maps collected from the

adhesive/dentin interface at the gingival margin of specimens stored in aqueous solution for 48 h and 90 days are presented in Figures 2 and 3, respectively. All spectra were recorded from 875 to 1785  $\text{cm}^{-1}$ , which spans the fingerprint region associated with adhesive, collagen, and mineral. The peaks associated with the adhesive occur at 1720  $\text{cm}^{-1}$  (carbonyl), 1609  $\text{cm}^{-1}$  (phenyl C=C), and 1113  $\text{cm}^{-1}$  (C—O—C), and the major peaks associated with the collagen appear at 1245  $\text{cm}^{-1}$  (amide III), 1273  $\text{cm}^{-1}$  (amide III), 1453  $\text{cm}^{-1}$  ( $\text{CH}_2$ ), and 1667  $\text{cm}^{-1}$  (amide I), respectively. Additional features associated with the collagen appear at 938  $\text{cm}^{-1}$  ( $\alpha$  backbone) and 921  $\text{cm}^{-1}$  (C=C stretch) and the spectral features associated with the mineral occur at 961 (P—O symmetric stretch) and 1072  $\text{cm}^{-1}$  ( $\text{CO}_3$ ), respectively.

As shown in Figures 2 and 3, the first spectrum was acquired from the pure adhesive. Peaks associated with the adhesive and collagen components of dentin were noted in the second spectrum. The Raman peak of the P—O group in the twelfth spectrum of the 48-h specimen suggested that this represented the bottom of the demineralized dentin layer. In the 90-day specimens (Figure 3), features associated with demineralized dentin collagen dominate the second through 13th spectra; note the very limited contribution from spectral features associated with the adhesive (1720 and 1609  $\text{cm}^{-1}$ ) beyond the second micrometer position. The spectra recorded at the second, fourth, and fifth micrometer positions of the interface are presented in detail, and major spectral changes have been marked with arrows (Figures 2 and 3). The intensity of the Raman bands associated with the adhesive decreased as a function of depth, indicating the gradual decline of adhesive penetration. At the fifth micrometer position, there is almost no contribution from spectral features associated with the adhesive. After water storage for 90 days, the relative intensity of the adhesive bands is reduced, indicating that there has been leaching of adhesive resin from the interfacial region. It was also noted that the relative intensity of the band at 1640  $\text{cm}^{-1}$  in the spectra recorded at the second and fourth micrometer positions was relatively high. This band is associated with the content of C=C bond, indicating that the degree of conversion is lower in the adhesive that penetrated into the demineralized zone.

The ratios of the relative integrated intensities of the spectral features from the mineral (961  $\text{cm}^{-1}$ , P—O) and collagen (1453,  $\text{CH}_2$ ) (mineral/matrix ratios) were used to determine the extent of dentin demineralization at the gingival margin (Figure 4). The depth, degree, and profile of dentin demineralization at the gingival margin of specimens stored for 48 h and 90 days were clearly seen. At the gingival margin, the depth of dentin demineralization was ~12–13  $\mu\text{m}$  for both the 48-h and 90-day specimens. To determine differences in adhesive penetration as a function of spatial position across the interface, the ratios of the relative integrated intensities of the spectral features associated with the adhesive and collagen were calculated. The C—O—C (1113  $\text{cm}^{-1}$ ) was used to monitor the adhesive concentration, and the amide I peak (1667  $\text{cm}^{-1}$ ) was selected for collagen. Figure 4 shows the ratios of 1113/1667 as a function of spatial position across the interface at the gingival margin of specimens stored for 48 h and 90 days. SB adhesive infiltrated about 4–5  $\mu\text{m}$  of the 12- $\mu\text{m}$  demineralized dentin in the 48-h specimen. In comparison, after 90 days of aqueous storage, SB adhesive infiltration was reduced to ~2  $\mu\text{m}$ .

The Raman spectra of unprotected collagen in the demineralized dentin layer after 48 h and 90 days of aqueous storage are compared in Figure 5. The spectral features are present at 1667 (amide I), 1453 (CH def), 1245 (amide III), 939 ( $\alpha$  backbone), and 921 (C—C stretch). Table I presents the ratios of the relative integrated peak areas of key features associated with the collagen. The amide I (C=O stretching vibration) mode is sensitive to the molecular conformation of the polypeptide chains.<sup>25,26</sup> The position and intensity of this band is typical of collagen fibril with triple helical structure. In comparing this region in the spectra of unprotected collagen, there is a relative increase in the ratios of Amide I/CH and Amide I/Amide III in the 90-day specimens. These spectral changes indicate that the ordered collagen

structure has become disorganized<sup>25,27,28</sup> The relative difference in intensity of these spectral features could be caused by a loosening of the collagen fibril structure from water absorption.<sup>29</sup>

## DISCUSSION

The hybrid layer has been described as the weakest link, that is, the “Achilles heel” of the adhesive/dentin bond.<sup>15</sup> This characterization is based on the results of several *in vitro* and *in vivo* investigations, which point to a breakdown of the hybrid layer in wet environments.<sup>15–17,30–32</sup> It was speculated that this degradation could be attributed to a variety of factors, including the leaching of unreacted monomers and oligomers as well as exposed demineralized dentin collagen. Authors of previous publications theorized that decreased tensile and shear bond strength values in adhesive/dentin interface specimens stored in aqueous media for 3–12 months can be attributed to incomplete adhesive polymerization.<sup>33</sup>

Two main reasons for the release of substances from polymeric materials are (1) unbound monomers or additives or both are extracted by solvents after polymerization; (2) leachable components are created by degradation or erosion over time.<sup>34</sup> In the degradation process, polymer chains are cleaved into oligomers, and finally, under specific conditions into monomers.<sup>34</sup> Polymer degradation may be associated with photo, thermal, mechanical, or chemical factors.

It is generally reported that methacrylate-based resins are polymerized to the extent of 50 – 75%; thus, there are unreacted methacrylate groups in these resins.<sup>35</sup> In addition, previous authors have suggested that the resin between collagen fibrils is not as well-polymerized, as resin immediately adjacent to the fibrils.<sup>36</sup> Under these conditions, the poorly polymerized resin within the demineralized dentin matrix may be slowly extracted by solvent. Wet bonding may also interfere with the polymerization of the adhesive that infiltrates the collagen network. Under the conditions associated with wet bonding, there is residual conditioner, solvent, water, and  $\text{Ca}^{2+}/\text{PO}_4^{3-}$  ions within the demineralized dentin matrix. The effect of these reagents on the polymerization of the adhesive within the demineralized dentin matrix has not been defined, but in test tubes, the monomer/polymer conversion of HEMA/BisGMA bonding resins decreases from 53.5 to 22.7% when 0.2 mL of water is added per milliliter of resin.<sup>37</sup> A related study showed that at water concentrations  $\geq 25$  vol %, SB adhesive/water solutions mimicked oil and water mixtures, in which they separated into distinct phases immediately following sonication.<sup>38</sup> At this concentration of water, the SB adhesive separates into distinct particles that are made up primarily of BisGMA; the matrix or material surrounding the particles is primarily HEMA. If a similar phenomenon occurs within the demineralized dentin matrix, the hybrid layer would be composed of isolated pockets of HEMA and BisGMA rather than a three-dimensional integrated polymer network.

The spectroscopic results in the present study suggest that, as a result of adhesive phase separation, nearly 70% of the demineralized intertubular dentin matrix at the gingival margin of these *in vitro* class II composite restorations is not protected by the critical dimethacrylate component (BisGMA). The dimethacrylate BisGMA is the formulation component, which contributes most to the crosslinked polymeric adhesive; the monomethacrylate HEMA cannot crosslink with itself and can only become part of a crosslinked system by copolymerizing with the BisGMA. Under these conditions, the hybrid layer is not the “ideal” three-dimensional integrated collagen/polymer network, instead, a portion of the hybrid layer will be only made of collagen that is protected by the hydrolytically unstable monomethacrylate HEMA.<sup>19,38</sup>

In the present study, distinct differences are noted in the adhesive infiltration patterns as a function of aging in aqueous solution. The spectral differences in adhesive infiltration in

concert with the similar depths of dentin demineralization provide direct evidence that there is compositional gradient with less of the bulky BisGMA/HEMA tied into the network than was originally present in the early stage. These results represent loss of adhesive monomers or oligomers from the interface during the 90 days of storage. The lower degree of conversion of adhesive that penetrated the demineralized layer provides direct evidence of incomplete polymerization and associated unreacted monomers and oligomers. These results provide the first direct evidence of leaching of monomers and oligomers from the adhesive/dentin interface formed at the gingival margin of class II composite restorations following aqueous storage.

Differences noted in the spectra recorded from unprotected collagen in the aged class II composite restorations quite likely reflect a loosening of the collagen fibril structure as a result of water absorption.<sup>29</sup> The amide I (C=O stretching vibration) mode is sensitive to the molecular conformation of the polypeptide chains.<sup>25,26</sup> The broadening and relative increase in intensity of the amide I feature in the 90-day specimens suggest disorder in the collagen.<sup>39</sup> The relative decrease in the intensity of the spectral feature associated with  $\alpha$  backbone would similarly support disordered arrangement in the collagen following aqueous storage. A change in collagen helicity is more likely associated with a change in the number of carbonyls that form hydrogen bonds with water.<sup>40,41</sup> In other words, loss of helicity in collagen could influence the water-protein interaction, and this change should consequently be reflected in the protein bands in the Raman spectra. For example relative decrease in the ratio of the features associated with  $\alpha$  backbone (939)/CH (1453) and relative increase in the amide I/CH and amide I/amide III ratios in the 90-day specimens.

These spectral results are in general agreement with recent high resolution morphologic investigations, which reported degradation of denuded, acid-etched collagen fibrils during aqueous aging.<sup>42,43,44</sup> In these studies, the degradation was noted in the absence of bacteria. Previous investigators have suggested that the degradation is linked to the slow release of proteolytic enzymes from the mineralized dentin matrix.<sup>42</sup>

In the mouth, clinicians have reported that there is frequently a gap between the composite and the tooth at the gingival margin of class II composite restorations.<sup>11</sup> When such a gap is present, it is quite likely that the adhesive/dentin interface at the gingival margin will be exposed to oral fluids as illustrated in Figure 6. On the basis of the results presented in the present study, these fluids would promote the degradation of hydrolytically unstable components in the adhesive. A direct consequence of this degradation would be exposure of the subjacent demineralized dentin matrix to oral fluids. With the degradation of the hydrolytically unstable components, approximately 10  $\mu\text{m}$  of collagen at the gingival margin would be exposed to oral fluids.

If water absorption occurs at the adhesive/dentin interface, there may be fluid movement at the junction of the adhesive resin and hybrid layer during flexing of the restoration and tooth.<sup>15</sup> On the basis of the investigation by Paul et al.,<sup>45</sup> this exchange of fluid could promote degradation of the HEMA-rich phase in a BisGMA/HEMA adhesive that undergoes phase separation in the presence of a hydrated demineralized dentin matrix. In the mouth, the network of collagen fibrils that had been infiltrated by the HEMA-rich phase would now be exposed to oral fluids. The exposed collagen could be attacked and degraded by bacterial enzymes.<sup>17, 46</sup> The cumulative effect would be breakdown of the adhesive/dentin bond, and ultimately, undermining of the marginal integrity of the composite restoration.

One of the primary requirements for any dentin bonding system is resistance to degradation in the oral environment.<sup>47</sup> This study provides direct evidence of the breakdown of hydrolytically unstable adhesive monomers or oligomers at the hybrid layer/dentin interface in class II composite restorations, following 90 days of aqueous aging. The results also provide direct

evidence of deterioration in the unprotected collagen at the gingival margin in the aged class II composite restorations. Two distinct advantages of micro-Raman spectroscopy are minimal sample preparation and nondestructive nature of this technique. By combining this method of analysis with an excitation source that minimizes the sample fluorescence, the adhesive/dentin sample can be studied without altering or damaging the interface. Because the technique is nondestructive, the same sample can be evaluated prior to and subsequent to storage.

### Acknowledgements

The authors express their sincere appreciation to the oral surgeons, who helped with the collection of teeth that were used in this study. This work is a contribution from the UMKC Center for Research on Interfacial Structure and Properties (UMKC-CRISP).

### References

1. Kidd EAM, Toffenetti F, Mjor IA. Secondary caries. *Int Dent J* 1992;42:127–138. [PubMed: 1500208]
2. Kidd EAM, Beighton D. Prediction of secondary caries around tooth-colored restorations: A clinical and microbiological study. *J Dent Res* 1996;75:1942–1946. [PubMed: 9033448]
3. Collins CJ, Bryant RW, Hodge KLV. A clinical evaluation of posterior composite resin restorations: 8-Year findings. *J Dent* 1998;26:311–317. [PubMed: 9611936]
4. Hunter AR, Treasure ET, Hunter AJ. Increases in cavity volume associated with the removal of class 2 amalgam and composite restorations. *Oper Dent* 1995;20:2–6. [PubMed: 8700763]
5. Van Meerbeek B, Vargas M, Satoshie I, Yoshida Y, Perdigao J, Lambrechts P, Vanherle G. Microscopy investigations. Techniques, results, limitations. *Am J Dent* 2000;13(special issue):3–18.
6. Mair LH. Ten-year clinical assessment of three posterior resin composites and two amalgams. *Quintessence Int* 1998;29:483–490. [PubMed: 9807127]
7. Nordbo H, Leirskar J, von der Fehr FR. Saucer-shaped cavity preparations for posterior approximal resin composite restorations: Observations up to 10 years. *Quintessence Int* 1998;29:5–11. [PubMed: 9611469]
8. Dunne SM, Gainsford ID, Wilson NHF. Current materials and techniques for direct restorations in posterior teeth. Part 1: Silver amalgam *Int Dent J* 1997;47:123–136.
9. Svanberg M, Mjor IA, Orstavik D. Mutans streptococci in plaque from margins of amalgam composite, and glass-ionomer restorations. *J Dent Res* 1990;69:861–864. [PubMed: 2109000]
10. Meiers JC, Kresin J. Cavity disinfectants and dentin bonding. *Oper Dent* 1996;21:153–159. [PubMed: 8957905]
11. Roulet JF. Benefits and disadvantages of tooth-coloured alternatives to amalgam. *J Dent* 1997;25:459–473. [PubMed: 9604577]
12. Hilton TJ. Cavity sealers, liners, and bases: Current philosophies and indications for use. *Oper Dent* 1996;21:134–146. [PubMed: 8957903]
13. Bergenholtz G, Cox CF. Bacterial leakage around dental restorations: Its effects on the dental pulp. *J Oral Path* 1982;11:439–450. [PubMed: 6819352]
14. Bullard RH, Leinfelder KR, Russell CM. Effect of coefficient of thermal expansion on microleakage. *J Am Dent Assoc* 1988;116:871–874. [PubMed: 3164741]
15. Sano H, Yoshikawa T, Pereira PNR, Kanemura N, Morigami M, Tagami J, Pashley DH. Long-term durability of dentin bonds made with a self-etching primer, *in vivo*. *J Dent Res* 1999;78:906–911. [PubMed: 10326735]
16. Burrow MF, Satoh M, Tagami J. Dentin durability after three years using a dentin bonding agent with and without priming. *Dent Mater* 1996;12:302–307. [PubMed: 9170998]
17. Hashimoto M, Ohno H, Kaga M, Endo K, Sano H, Oguchi H. *In vivo* degradation of resin–dentin bonds in humans over 1 to 3 years. *J Dent Res* 2000;79:1385–1391. [PubMed: 10890717]
18. Wang Y, Spencer P. Quantifying adhesive penetration in adhesive/dentin interface using confocal Raman microspectroscopy. *J Biomed Mater Res* 2002;59:46–55. [PubMed: 11745536]
19. Wang Y, Spencer P. Hybridization efficiency of the adhesive dentin interface with wet bonding. *J Dent Res* 2003;82:141–145. [PubMed: 12562889]

20. Spencer P, Wang Y, Walker MP, Wieliczka DM, Swafford JR. Interfacial chemistry of the dentin/adhesive bond. *J Dent Res* 2000;79:1458–1463. [PubMed: 11005728]
21. Spencer P, Swafford JR. Unprotected protein at the dentin-adhesive interface. *Quintessence Int* 1999;30:501–507. [PubMed: 10635264]
22. Sano H, Takatsu T, Ciucchi B, Horner JA, Matthews WG, Pashley DH. Nanoleakage: Leakage within the hybrid layer. *Oper Dent* 1995;20:18–25. [PubMed: 8700762]
23. Bean TA, Zhuang WC, Tong PY, Eick JD, Yourtee DM. Effect of esterase on methacrylates and methacrylate polymers in an enzyme simulator for biodurability and biocompatibility testing. *J Biomed Mater Res* 1994;28:59–63. [PubMed: 8126029]
24. Cannon MJ, Kostoryz E, Russo KA, Smith RE, Yourtee DM. Bisphenol A and its biomaterial monomer derivatives alteration of in vitro cytochrome P450 metabolism in rat, minipig and human. *Biomacromolecules* 2000;1:656–664. [PubMed: 11710196]
25. Goheen SC, Lis LJ, Kauffman JW. Raman spectroscopy of intact feline corneal collagen. *Biochim Biophys Acta* 1978;536:197–204. [PubMed: 708760]
26. Frushour BG, Koenig JL. Raman scattering of collagen, gelatin, and elastin. *Biopolymers* 1975;14:379–391. [PubMed: 1174668]
27. Rengopalakrishnan V, Carreira LA, Collette TW, Dobbs JC, Chandraksasan G, Lord RC. Non-uniform triple helical structure in chick skin type I collagen on thermal denaturation: Raman spectroscopic study. *Z Naturforsch [C]* 1998;53:383–388.
28. Sane SU, Cramer SM, Przybycien TM. A holistic approach to protein secondary structure characterization using amide I band Raman spectroscopy. *Anal Biochem* 1999;269:255–272. [PubMed: 10221997]
29. Farrell RA, McCauley RL. On corneal transparency and its loss with swelling. *J Opt Soc Am* 1976;66:343–345.
30. Budevskva BO, Sum ST, Jones TJ. Application of multivariate curve resolution for analysis of FT-IR microspectroscopic images of in situ plant tissue. *Appl Spectrosc* 2003;57:124–131. [PubMed: 14610947]
31. Hashimoto M, Tay FR, Ohno H, Sano H, Kaga M, Yiu C, Kumagai H, Kudou Y, Kubota M, Oguchi H. SEM and TEM analysis of water degradation of human dentinal collagen. *J Biomed Mater Res Part B: Appl Biomater* 2003;66:287–298. [PubMed: 12808586]
32. Hashimoto M, Ohno H, Sano H, Tay FR, Kaga M, Kudou Y, Oguchi H, Araki Y, Kubota M. Micromorphological changes in resin–dentin bonds after 1 year of water storage. *J Biomed Mater Res Part B: Appl Biomater* 2002;63:306–311.
33. Kiyamura M. Bonding strength to bovine dentin with 4-META/MMA-TBB resin. Long term stability and influence of water. *J Jpn Dent Mater* 1987;6:860–872.
34. Van Krevelen, DW. *Properties of Polymers*. New York: Elsevier; 1997. p. 641-660.
35. Peutzfeldt A. Resin composites in dentistry: The monomer systems. *Eur J Oral Sci* 1997;105:97–116. [PubMed: 9151062]
36. Pashley DH, Carvalho RM. Dentine permeability and dentine adhesion. *J Dent* 1997;25:355–372. [PubMed: 9241954]
37. Jacobsen T, Soderholm K-J. Some effects of water on dentin bonding. *Dent Mater* 1995;11:132–136. [PubMed: 8621034]
38. Spencer P, Wang Y. Adhesive phase separation at the dentin interface under wet bonding conditions. *J Biomed Mater Res* 2002;62:447–456. [PubMed: 12209931]
39. Wang Y, Spencer P. Analysis of acid-treated dentin smear debris and smear layers using confocal Raman microspectroscopy. *J Biomed Mater Res* 2002;60:300–308. [PubMed: 11857437]
40. Payne KJ, Veis A. Fourier transform IR spectroscopy of collagen and gelatin solutions: Deconvolution of the amide I band for conformational studies. *Biopolymers* 1988;27:1749–1760. [PubMed: 3233328]
41. Vyavahare N, Ogle M, Schoen FJ, Zand R, Gloeckner DC, Sacks M, Levy RJ. Mechanisms of bioprosthetic heart valve failure: Fatigue causes collagen denaturation and glycosaminoglycan loss. *J Biomed Mater Res* 1999;46:44–50. [PubMed: 10357134]



42. Pashley DH, Tay FR, Yiu C, Hashimoto M, Breschi L, Carvalho RM, Ito S. Collagen degradation by host-derived enzymes during aging. *J Dent Res* 2004;83:216–221. [PubMed: 14981122]
43. De Munck J, Van Meerbeek B, Yoshida Y, Inoue S, Suzuki K, Lambrechts P. Four-year water degradation of a resin-modified glass-ionomer adhesive bonded to dentin. *Eur J Oral Sci* 2004;112:73–83. [PubMed: 14871197]
44. Armstrong SR, Vargas MA, Chung I, Pashley DH, Campbell JA, Laffoon JE, Qian F. Resin–dentin interfacial ultrastructure and microtensile dentin bond strength after five-year water storage. *Oper Dent* 2004;29:705–712. [PubMed: 15646228]
45. Paul SJ, Leach M, Rueggeberg FA, Pashley DH. Effect of water content on the physical properties of model dentine primer and bonding resins. *J Dent* 1999;27:209–214. [PubMed: 10079627]
46. Sorsa T, Ingman T, Suomalainen K, Haapasalo M, Kontinen Y, Lindy O, Saari H, Uitto V. Identification of proteases from periodontopathogenic bacteria as activators of latent human neutrophil and fibroblast-type interstitial collagenases. *Infect Immun* 1992;60:4491–4495. [PubMed: 1398963]
47. Kugel G, Ferrari M. The science of bonding: From first to sixth generation. *J Am Dent Assoc* 2000;131:20S–25S. [PubMed: 10860341]

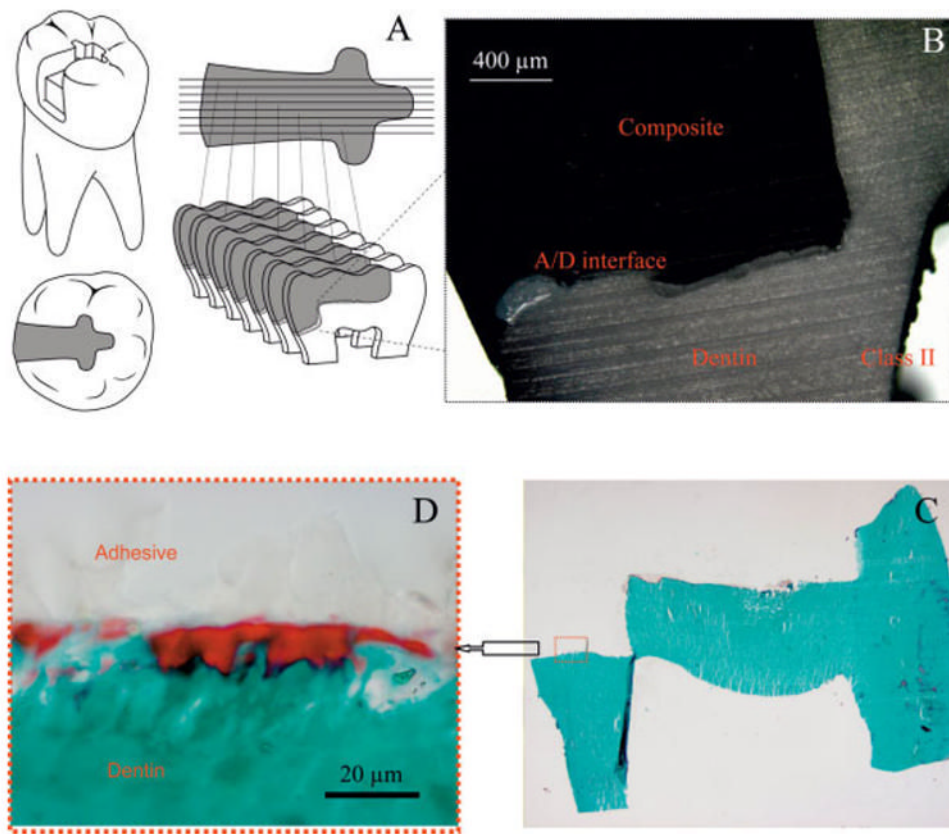


**Figure 1.** Light microscopic picture of the adhesive/dentin interfaces of the proximal and gingival walls of class II composite restorations. [Color figure can be viewed in the online issue, which is available at [www.interscience.wiley.com](http://www.interscience.wiley.com).]

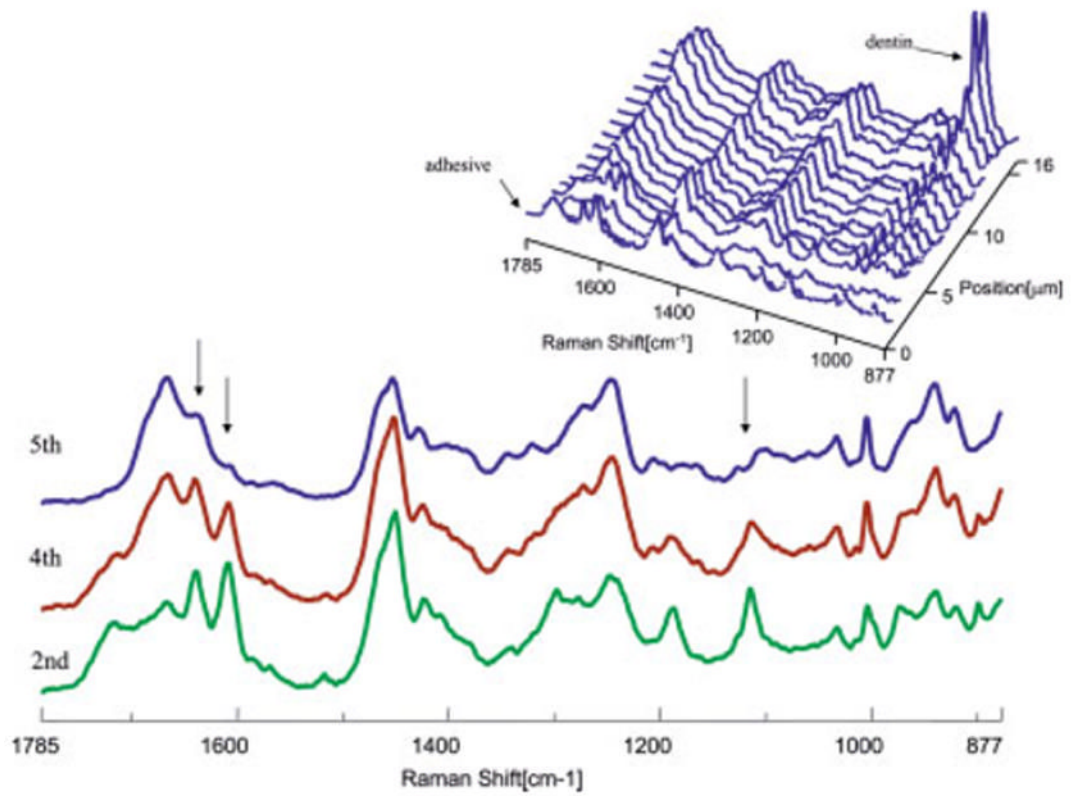


**Figure 2.**

Micro-Raman mapping spectra acquired at 1- $\mu\text{m}$  intervals across SB adhesive/dentin interface at gingival margin (for 48 h of aqueous storage). [Color figure can be viewed in the online issue, which is available at [www.interscience.wiley.com](http://www.interscience.wiley.com).]

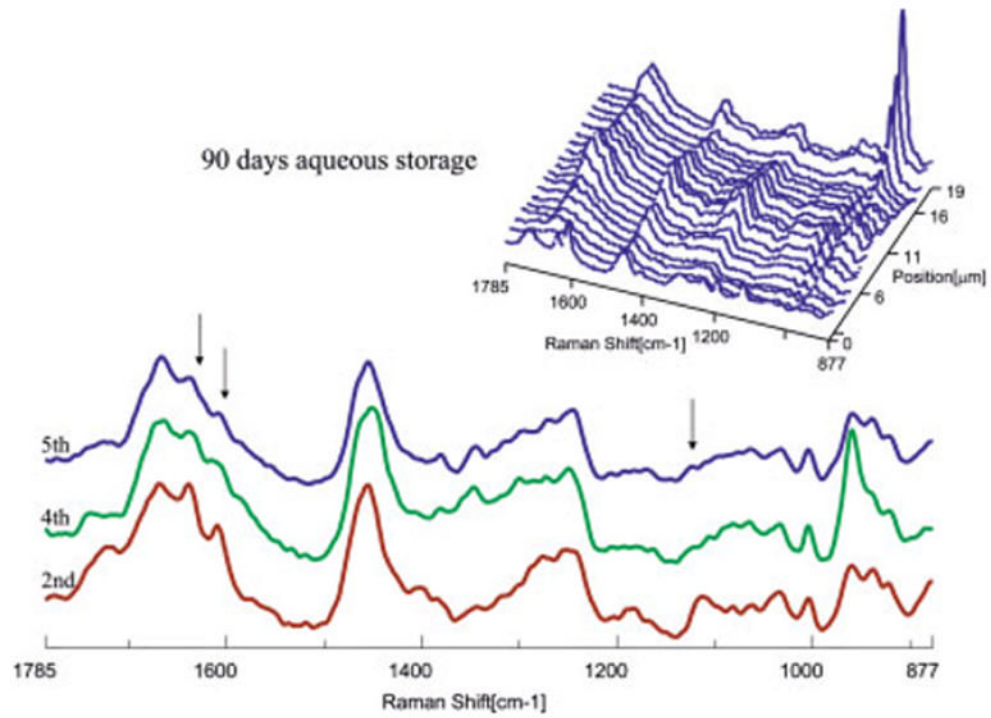


**Figure 3.** Micro-Raman mapping spectra acquired at 1- $\mu\text{m}$  intervals across SB adhesive/dentin interface at gingival margin (for 90 days of aqueous storage). [Color figure can be viewed in the online issue, which is available at [www.interscience.wiley.com](http://www.interscience.wiley.com).]

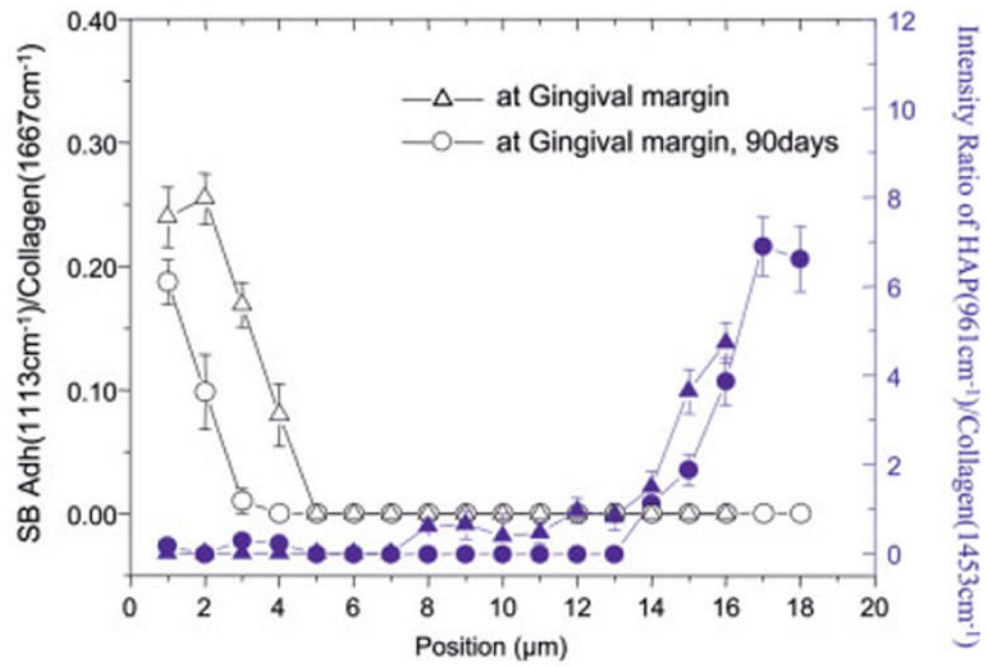


**Figure 4.** Adhesive penetration and degree of demineralization as a function of depth at gingival margins (for 48 h versus 90 days of aqueous storage). [Color figure can be viewed in the online issue, which is available at [www.interscience.wiley.com](http://www.interscience.wiley.com).]

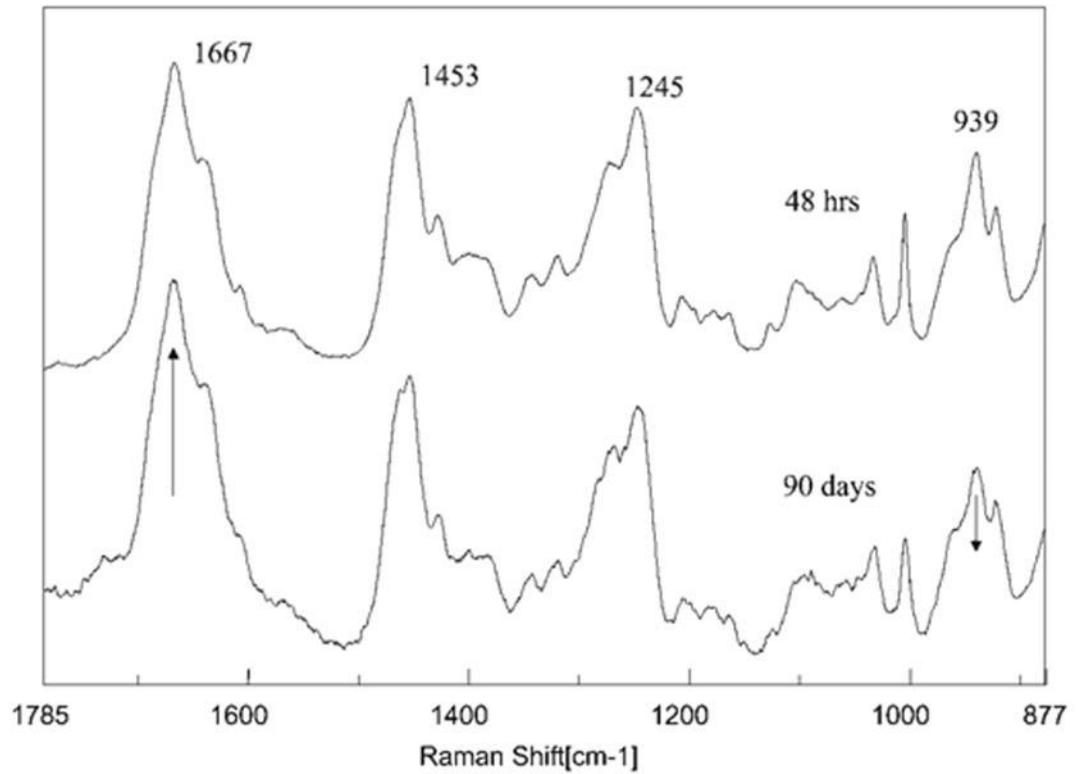


**Figure 5.** Raman spectra of dentin collagen recorded in the exposed collagen region at the adhesive/dentin interface (for 48 h versus 90 days of aqueous storage).

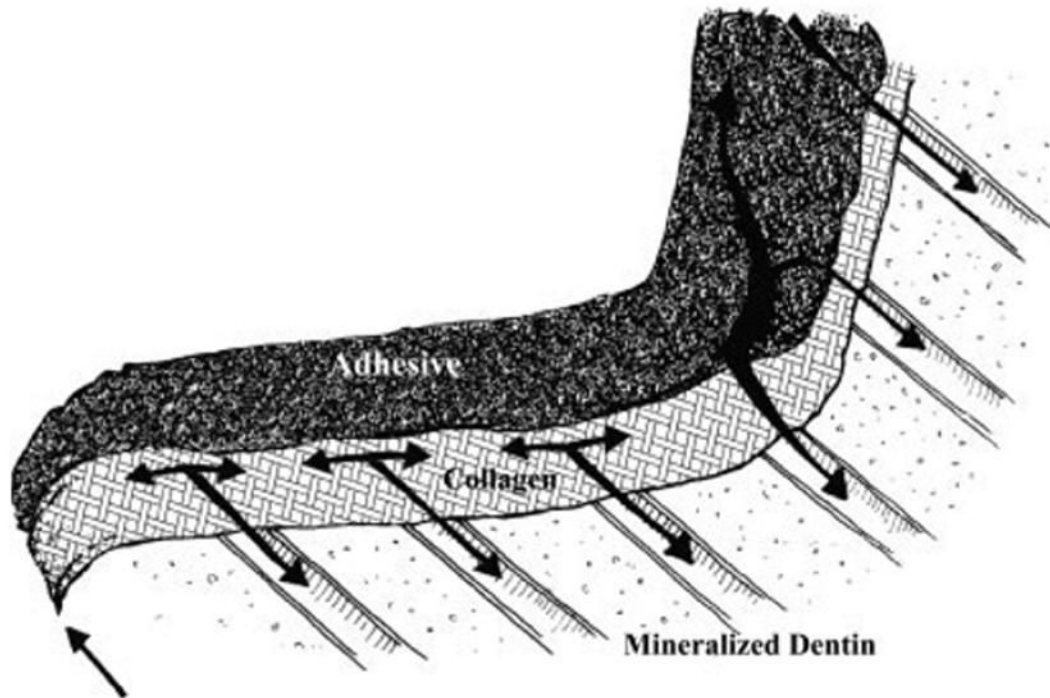


**Figure 6.**

Crosssectional illustration of gingival seat of class II composite restoration. ↑ arrow indicates migration of oral fluid at gingival margin. ↓ arrows indicate movement of oral fluid through demineralized dentin (collagen) matrix that has been exposed as a result of hydrolytic breakdown of the HEMA-rich phase. In this illustration, the resin tags are not visible, because they are embedded below the plane of observation.

**TABLE I**  
Relative Ratios of Micro-Raman Spectral Bands<sup>a</sup>

	1667/1453	1667/1245	939/1453	939/921 <sup>b</sup>
48 h	1.23	1.34	1.61	0.68
90 days	1.52	1.63	1.28	0.57

<sup>a</sup> Integrated band areas were calculated using a two-point base method.

<sup>b</sup> Curve fitting was used to separate these two bands.